

1 **Photobleaching of Red Fluorescence in Oral Biofilms**

2 C. K. Hope,*¹ E. de Josselin de Jong,^{1,2} M. R. T. Field,³ S. P. Valappil,¹ and S. M.
3 Higham¹

4

5 ¹School of Dental Sciences, University of Liverpool, UK

6 ²Inspektor Research Systems BV, Amsterdam, Netherlands

7 ³Department of Human Anatomy and Cell Biology, University of Liverpool, UK

8

9 ***Corresponding Author:**

10 Dr Chris Hope, University of Liverpool, School of Dental Sciences, Research Wing,
11 Daulby Street, Liverpool. United Kingdom, L69 3GN. Tel: +44(0) 151 706 5296
12 Email: chope@liv.ac.uk

13

14 **Key Words:**

15 Oral biofilm, plaque, fluorescence, quantitative light-induced fluorescence digital
16 (QLFD), porphyrin, photobleaching

17

18

19 **Abstract**

20 *Background and Objective:* Many species of oral bacteria can be induced to
21 fluoresce due to the presence of endogenous porphyrins, a phenomenon that can be
22 utilised to visualise and quantify dental plaque in the laboratory or clinical setting.
23 However; an inevitable consequence of fluorescence is photobleaching, and the
24 effects of this on longitudinal, quantitative analysis of dental plaque has yet to be
25 ascertained.

26 *Material and Methods:* Filter membrane biofilms were grown from salivary inocula or
27 single species (*Prevotella nigrescens* and *Prevotella intermedia*). The mature
28 biofilms were then examined in a custom-made lighting rig comprising of 405 nm
29 light emitting diodes capable of delivering 220 W m^{-2} at the sample, an appropriate
30 filter and a digital camera; a set-up analogous to quantitative light-induced
31 fluorescence digital (QLFD). Longitudinal sets of images were captured and
32 processed to assess the degradation in red fluorescence over time.

33 *Results:* Photobleaching was observed in all instances. The highest rates of
34 photobleaching were observed immediately after initiation of illumination, specifically
35 during the first minute. Relative rates of photobleaching during the first minute of
36 exposure were; 19.17, 13.72, and 3.43 (arbitrary units per minute) for *P. nigrescens*
37 biofilms, microcosm biofilm and *P. intermedia* respectively.

38 *Conclusion:* Photobleaching could be problematic when making quantitative
39 measurements of porphyrin fluorescence *in situ*. Reducing both light levels and
40 exposure time, in combination with increased camera sensitivity, should be the
41 default approach when undertaking analyses by QLFD.

42 **Introduction**

43 **Porphyrins and oral bacteria**

44 Fluorescent porphyrins are present in many members of our indigenous microbiota
45 (1, 2), including those found in the oral cavity (3-5). Whilst many bacterial porphyrins
46 are associated with photosynthesis, a relatively large amount of haem (iron
47 protoporphyrin IX) for example is incorporated on the cell surface of the putative
48 periodontal pathogen *Porphyromonas gingivalis* to protect it from hydrogen peroxide
49 (6) with similar processes occurring in *Prevotella nigrescens* and *Prevotella*
50 *intermedia* (7) (both formerly classified as *Bacteroides melanogenicus*) (8) . The
51 molecular fluorescence of bacterial porphyrins is an adventitious phenomenon which
52 results from the absorption of a photon and the subsequent re-emission of another
53 photon of a longer wavelength as the electrons in the molecule return from the
54 excited (triplet) state to the ground state. Specific porphyrins have distinct excitation
55 spectra with different maxima; protoporphyrin at 593 nm and coproporphyrin 604 nm
56 (9). The wavelengths suitable for the efficient fluorescent excitation of bacterial
57 porphyrins range from near ultraviolet (300 nm) to blue (450 nm). The discrepancy
58 between the colour of the incident light and the fluorescent emission, a phenomenon
59 known as the Stokes shift (10), allows for the selective capture and quantification of
60 the emitted light via an appropriate filter set-up.

61

62 Photobleaching occurs when a fluorophore is irreversibly damaged so that it no
63 longer fluoresces. Although the exact mechanisms by which photobleaching occur
64 are not clear, it has been suggested that the fluorophores undergo an oxidative
65 reaction with highly reactive oxygen species such as singlet oxygen ($^1\text{O}_2$) and

66 hydroxyl radicals (OH·) (11). Molecules already in the excited (singlet) state can also
67 be destructively excited by an additional excitation photon, an event dubbed two-
68 photon excitation, but it is unlikely that this process would occur in the experiments
69 discussed herein. Other results have demonstrated photobleaching reactions
70 occurring between excited dye molecules (12) . The generation of highly reactive
71 oxygen species has also been demonstrated to cause cell death in *P. gingivalis*, *P.*
72 *nigrescens* and *P. intermedia* by the excitation of endogenous porphyrins (13).
73 Lethal photosensitisation (photodynamic therapy) either by the application of
74 photosensitising agents or via endogenous porphyrins has the potential to be an
75 effective means of treating plaque-related diseases (14) .

76

77 Fluorescence microscopy techniques can utilise the kinetics of photobleaching by
78 fluorescence loss in photobleaching (FLIP) and fluorescence recovery after
79 photobleaching (FRAP) to reveal rates of diffusion within cell membranes, organelles
80 (15) and biofilms (16). However, when undertaking quantitative measurements of
81 fluorescence, photobleaching can be problematic (17).

82

83 **Quantitative light-induced fluorescence**

84 Quantitative Light-induced Fluorescence (QLF) uses violet light to induce
85 fluorescence in tooth enamel and collects the resulting emissions via a high band-
86 pass filter (>520 nm) in conjunction with a computer-controlled digital camera (18).
87 When viewed under QLF lighting conditions, areas of demineralised enamel
88 fluoresce less than surrounding sound enamel and so appear darker. Regions of

89 demineralised enamel are visible under QLF lighting conditions before they are
90 visible to the eye as white spot lesions (19). Although QLF was initially developed
91 for the analysis of tooth enamel (20), it has been subsequently demonstrated to be
92 capable of revealing dental plaque due to the fluorescence of endogenous
93 porphyrins (5). However, since the filter configuration of QLF was designed to
94 maximise the transmission of green light there are limitations as to its usefulness for
95 the analysis of dental plaque (21). Quantitative Light-Induced Fluorescence Digital
96 (QLFD) is an adaptation of QLF which employs a modified filter set (D007, Inspektor
97 Research Systems BV, Amsterdam, Netherlands), narrow-band violet light (405 nm)
98 and a high-specification digital SLR camera. This configuration has been specifically
99 developed to enhance the visualisation and quantification of plaque. During clinical
100 investigations to assess plaque, QLFD is typically used to identify regions of red
101 fluorescence and capture a sequence of images at different visits in order to quantify
102 the progression of conservative dental treatment.

103 A better understanding of photobleaching phenomena with respect to indigenous
104 bacterial porphyrins, illuminated by QLFD lighting, *in situ* is required to enable
105 accurate quantitative analyses of dental plaque to be undertaken.

106

107 **Materials and Methods**

108 **Filter membrane biofilms**

109 Approximately 10 ml of unstimulated saliva was obtained from a healthy volunteer
110 with no previous history of periodontitis. This was split into 1 ml aliquots and frozen.
111 Nitrocellulose filter-membranes (47 mm diameter, 0.45 µm pore size, Invitrogen Ltd.,

112 Paisley, Renfrewshire, UK) were laid, with their inked grid upwards, on top of blood
113 agar (Oxoid, Basingstoke, UK) supplemented with 5% defibrinated horse blood. A
114 50 µl aliquot of the saliva sample was spread over the membrane before being
115 incubated at 37°C in anaerobic conditions (80% N₂, 10% CO₂, 10% H₂) for seven
116 days to allow microcosm oral biofilms to develop. Individual biofilm laden filter
117 membranes were removed from the supporting agar and placed in a Petri dish which
118 had first had 200 µl of phosphate buffered saline (PBS) beaded over the surface to
119 help prevent the membrane biofilm from drying out. Similar single-species biofilms
120 were grown using heavy colony inocula of *Prevotella nigrescens* (ATCC 25261)
121 (seven day old cultures) or *Prevotella intermedia* (ATCC 25611) (five day old
122 cultures) suspended in 1 ml of PBS.

123

124 **Fluorescence imaging**

125 A custom-made rig, incorporating QLFD technology, was constructed to enable the
126 capture of fluorescent images under reproducible lighting conditions from surface-
127 mounted indium gallium nitride light emitting diodes (LED) (EWC 400 SC2C, radiant
128 power 600 mW, 23° beam angle; E Wave Corporation, London, UK) with a
129 wavelength band from 400 nm to a peak output at 405 nm (violet). To construct the
130 QLFD *in vitro* rig, an LED was soldered onto the outside of a copper ring, being a
131 section of standard domestic plumbing material, which acted as a heat-sink to
132 prevent overheating. Three such mounted LEDs were then fixed inside an
133 approximately hemispherical plastic bowl so that the light beams converged on the
134 sample (Figure 1). A hole was cut into the base for the unimpeded viewing of the
135 sample by a camera, with another hole in the sidewall to allow the sample to be

136 easily manipulated. The LEDs were powered by a DC adaptor with an output of 5
137 volts at 1.2 amps connected in parallel. The distance between the LEDs and the
138 sample was 100 mm at an angle of incidence between camera and LEDs of 30° from
139 the surface normal. The light incident on the sample was measured as irradiance by
140 a photosynthetically active radiometer (PAR) with a cosine corrected detector (Q201
141 PAR with SD221Q Cos detector, Macam Photometrics Limited, Livingston, UK). A
142 cut-off filter (D007, Inspektor Research Systems BV, Amsterdam, Netherlands) was
143 placed in front of the camera lens to minimise the transmission of light close to the
144 excitation wavelength whilst maximising the transmission of the red part of the
145 spectrum. All illumination / photobleaching experiments were undertaken in a dark-
146 room.

147

148 Images were captured with a 'live view' enabled digital SLR camera, (Model: 1000D,
149 Canon, Tokyo, Japan) equipped with a 60 mm, *f*/2.8 macro lens (Model: EF-S,
150 Canon) connected to a computer. Proprietary software (C2 v1.0.0.7, Inspektor
151 Research Systems BV) was used to control the camera and store the images. Low
152 apertures (i.e. *f*/2.8 to *f*/8) and ISO settings of 200 – 400 were typically used to
153 maximise the light sensitivity of the camera without adversely affecting image quality.
154 The camera's on-board 'custom white balance' feature was calibrated against a
155 sheet of white paper before fluorescence imaging to effectively eliminate the
156 colouration of the filter in the resulting images. The camera resolution was set to
157 'low' (3.4 megapixels) to facilitate the processing of large numbers of data files in the
158 form of uncompressed 24-bit bitmap files. The LEDs were switched on for at least
159 10 minutes prior to use to allow their temperature to stabilise. Without moving the
160 sample, or changing camera settings, a series of images was captured over time

161 using the in-built image sequencer incorporated into the control software. Control
162 experiments included membranes that were partially covered with aluminium foil to
163 shield portions of them from the light. Four separate microcosm biofilm
164 photobleaching experiments were undertaken whilst the experiments for single
165 species were conducted in duplicate.

166

167 **Image analysis**

168 Images were analysed with an open source software package (ImageJ 1.43q, The
169 National Institutes of Health, Bethesda, Maryland, USA, <http://rsb.info.nih.gov/ij/>).

170 The images comprising the time-lapse sequence were opened with ImageJ and
171 compiled into a single image 'stack'. The stack was then split into its red, green and
172 blue (RGB) component colour channels; to isolate the red channel as an 8-bit
173 greyscale (i.e. pixel brightness values from 0 to 255). A user-defined 'rectangular
174 selection' region of interest (ROI) was created within one of the inked grid squares
175 on the filter membrane. The size of the grid squares was 4 mm x 4 mm and the ROI
176 encompassed approximately 20 000 pixels. The 'z-axis profile' of the ROI was then
177 measured through the image stack and the mean pixel brightness values at each
178 time point were copied into Microsoft Excel. The ROI was then moved to an
179 adjacent square on the grid and the process repeated to give a total of eight discrete
180 counts from the same biofilm sample. The mean pixel brightness values from the
181 eight sample sights from the were then themselves averaged before being
182 normalised to 100 at time zero to yield the arbitrary unit used throughout these
183 experiments; 'normalised mean pixel brightness' (NMPB), which allowed the direct
184 comparisons to be made between separate experiments.

185

186 Changes in fluorescence (ΔF) were calculated in terms of the shift in NMPB per unit
187 time to yield results in terms of ΔF per minute. These ΔF values were then allocated
188 into sub-sets to determine mean ΔF between discrete time points within the
189 photobleaching experiment; from 0 to 1 minute, 1 to 2 minutes, 2 to 5 minutes, 5 to
190 10 minutes and 10 to 20 minutes.

191

192 **Inter-operator reliability**

193 Two researchers (CKH and MRTF) independently analysed the image stacks from
194 two photobleaching experiments in order to ascertain the reliability of the methods
195 previously described. This exercise was undertaken in light of the possible variability
196 due to manual selection of the ROI parameters; namely: size of ROI, placement of
197 ROI within the membrane square and choice of the eight membrane squares used
198 for analysis. Results were tested using Pearson Correlation with PASW Statistics
199 17.0 (equivalent to SPSS) (Polar Engineering and Statistics).

200

201 **Results**

202 **Light exposure**

203 The configuration of the LEDs at an angle of incidence to the sample of 30° (Figure
204 1) corresponded to a radiant intensity of 0.87 per unit solid angle (Lambert's cosine
205 law). The angle of incidence was within the angular response parameters of the
206 cosine corrected PAR detector. The maximum radiometer reading at the sample

207 location was $750 \mu\text{mol m}^{-2} \text{s}^{-1}$, which is equivalent to 220 W m^{-2} at 405 nm. Light
208 leakage from the LEDs was minimal, being measured at $1.8 \mu\text{mol m}^{-2} \text{s}^{-1}$
209 immediately outside the obvious pool of light from a single LED. Due to the build-up
210 of heat during operation, the LED's light output dropped to 89% of their initial power
211 after 10 minutes usage after which time their output stabilised (data not shown).

212

213 **Biofilm photobleaching**

214 Photobleaching was evident in all of the samples analysed in this study; microcosm
215 oral biofilm, *P. nigrescens* and *P. intermedia* single-species biofilms. A control
216 experiment was designed to confirm that light was responsible for the reduction in
217 fluorescence in which half of the sample was shielded from direct illumination with
218 aluminium foil. After 25 minutes, the NMPB on the exposed half dropped to 31.23
219 whilst the covered half was 84.73 (figure 2).

220

221 Figure 3 shows the results from an individual QLFD experiment which demonstrates
222 photobleaching as a decrease in NMPB over time. NMPB data such as these were
223 collated to yield means along with their corresponding standard deviations (Figure
224 4).

225

226 Rates of photobleaching, expressed as ΔF were highest during the initial stages of
227 exposure to light (i.e. the first minute). In the case of microcosm biofilms and *P.*
228 *nigrescens* biofilms, photobleaching rates fell to approximately half their initial value
229 after 10 minutes exposure (Figure 5). Initial rates of photobleaching during the first

230 minute of exposure, expressed as ΔF (arbitrary units normalised to 100 at time zero)
231 per minute, were; 19.17, 13.72, and 3.43 for *P. nigrescens* biofilms, microcosm
232 biofilm and *P. intermedia* respectively. Photobleaching dynamics were reproducible
233 between replicate samples; Pearson correlation coefficient values between the four
234 microcosm biofilm samples ranged from 0.993 to 0.997 and were significant at the
235 0.01 level (2-tailed).

236

237 **Inter-operator reliability**

238 Pearson correlation coefficients for the two photobleaching experiments subjected to
239 inter-operator reliability testing were significant at the 0.01 level (2-tailed) with
240 correlations of 0.992 and 1. The data presented herein was the first set of data that
241 was analysed.

242

243 **Discussion**

244 **Light exposure**

245 A PAR detector was chosen to measure the light irradiance from the custom rig
246 since photobleaching is dependent on the amount of light energy incident per unit
247 surface area and not the power output of the LEDs *per se* (22). The camera / image
248 analysis method of quantifying pixel brightness proved far more sensitive to subtle
249 changes in ambient lighting conditions than the results from the PAR detector would
250 have suggested. The data collected from the automated image sequencer yielded
251 fewer perturbations in the fluorescence curve than when captured manually during
252 preliminary experiments. This suggested that variation in lighting from the laptop

253 screen, reflected off the white laboratory coat worn by the operator, was detectable
254 in the analysed images. The inter-operator reliability data suggests that the image
255 analysis methods employed were robust and reproducible.

256

257 Whilst every effort was made to focus the light onto the centre of the filter
258 membrane, an *ad-hoc* observation made using the PAR revealed that a single
259 representative attempt to place the detector in the 'bright centre of the light beams'
260 by the unaided eye, yielded only 73% of the actual maximum irradiance obtainable
261 by scrutinising the meter readings. The difference between these two positions was
262 of the order of 10 mm. Although the foci of the LEDs were generally convergent
263 onto the sample, it is unclear how the extent of photobleaching relates to specific
264 positions within the pool of light incident on the sample. For example, an area with
265 less light incident upon it, will fluoresce less and will likewise have a lower rate of
266 photobleaching (23). The net result of this would be differential rates of
267 photobleaching across a (large) sample and a hypothetical example of this effect is
268 demonstrated in Figure 6. Performing image analysis on adjacent sites on the
269 biofilm membrane will help to minimise the effects of heterogeneous lighting.
270 Another confounding factor that should be considered is the photo-shielding effect
271 (24) which occurs when a relatively high concentration of fluorophore absorbs
272 excitation photons, which in turn reduces the number of photons able to penetrate
273 into deeper layers of the sample. 'Iron porphyrin' can account for up to 50% of the
274 dry weight of the biomass of *Bacteroides* (many of which have been reclassified as
275 *Prevotella spp.*) when growing on blood agar (25) . Photo-shielding could reduce the
276 observed effects of photobleaching due to decreased excitation within the sample as
277 a whole; in other words, there may not be a direct relationship between fluorescence

278 intensity / photobleaching and net porphyrin concentration within a heterogeneous,
279 three-dimensional microbial biofilm.

280

281 **Biofilm photobleaching**

282 Rates of photobleaching decreased during exposure to QLFD light for 20 minutes,
283 after which time there was very little further reduction in observed fluorescence. It is
284 unlikely that imaging (exposure) times beyond this would be representative of image
285 capture *in vivo*. A reduction in mean pixel brightness of ~14% after one minute's
286 illumination with QLFD represents an unacceptable inaccuracy for the quantitative
287 analysis of the red fluorescence of dental plaque. Casual viewing and manipulation
288 of a sample / patient under the 405 nm lighting in order to correct the focus,
289 determine other camera settings and image capture will inevitably cause
290 photobleaching. In order to minimise this effect, samples should be positioned and
291 focussed under normal, white-light conditions. It is however an unavoidable fact that
292 in order to observe fluorescence, one must perturb fluorescence.

293

294 The rates of ΔF observed suggest that this effect was immediate and replicated the
295 photobleaching kinetics of protoporphyrin IX previously observed in PLC hepatoma
296 cells at 405 nm (26). In the current study, ΔF values were grouped to yield average
297 values for all data points within discrete time bands (0 to 1 minutes, 1 to 2 minutes, 2
298 to 5 minutes, 5 to 10 minutes and 10 to 20 minutes) to obviate the confounding
299 effects of individual data points with a positive ΔF value amongst predominantly
300 negative ΔF (i.e. fluorescence decreasing) values. During a longitudinal study, a

301 system whereby the LEDs are only illuminated during imaging should be employed.
302 This will also maximise the power output of the LEDs as they emit more light when
303 they are at ambient (room) temperature as opposed to once they have warmed to
304 their operating temperature. Using the PAR detector it was determined that the
305 irradiance supplied by the lighting rig did not decrease due to heating effects when
306 operated for 5 seconds out of every minute, similarly lighting for 5 seconds out of
307 every 30 seconds only reduced light output to 99.45% (data not shown).

308

309 The differential fluorescence of oral anaerobic bacteria under ultraviolet light has
310 been suggested as a tool for their rapid identification. The fluorescence previously
311 observed in strains of *Bacteroides* (now reclassified as *Prevotella spp.* and *P.*
312 *gingivalis*) encompasses a colour range that has been described as; red, yellow, red-
313 orange, brilliant red, pink-orange, orange, yellow-orange, and red-brown (27) .
314 These colours also changed with age of the culture and are almost certainly a
315 manifestation of the sequential metabolism of porphyrins (28) . No fluorescence was
316 observed in *P. gingivalis* at any time, including when emulsified in methanol – a
317 technique which can reveal fluorescence in older cultures which have lost this
318 capacity (2) . The inability of *P. gingivalis* to fluoresce is probably due to the
319 deposition of haem as an μ -oxo dimer on the cell surface, as opposed to the
320 monomeric form in *Prevotella* (6, 7). It was observed in preliminary experiments that
321 the fluorescence of *P. intermedia* was greatly diminished when incubated for seven
322 days, hence the use of younger (five day) cultures.

323

324 An additional experiment was conducted to see if it was possible to use a biofilm-
325 laden filter membrane as a rudimentary photographic plate to create a recognisable
326 image. An acetate mask depicting the University of Liverpool logo was placed in
327 front of a microcosm biofilm and exposed to QLFD light. After 16 minutes, the mask
328 was removed to reveal a photobleached logo on the membrane (see supplementary
329 information).

330

331 Fluorescence imaging has the potential to be a useful tool for quantifying dental
332 plaque in the research environment, both in terms of the amount of fluorescent
333 material and the 'quality' of its fluorescent properties in terms of red and green
334 fluorescence (29). The methodology described herein for measuring photobleaching
335 of red fluorescence in microbial biofilms appears to be robust and reproducible.
336 However; the destruction of the endogenous fluorophores within dental plaque by
337 photobleaching phenomena, when viewed with QLFD or similar technologies, needs
338 to be considered and steps taken to curtail this effect in both the research and
339 clinical environments such as improving camera sensitivity (i.e. low shutter speeds,
340 low apertures and high ISO settings), filter characteristics and keeping irradiance to
341 a minimum. The reported studies do not imply that this technique has clinical
342 applicability, but provides proof of principle data. Issues such as biofilm thickness
343 and degree of pigmentation may influence the penetration of both the excitation and
344 emitted fluorescent light and therefore the rate of photobleaching *in vivo*. Further
345 research is required to determine the effects of photobleaching on plaque
346 fluorescence.

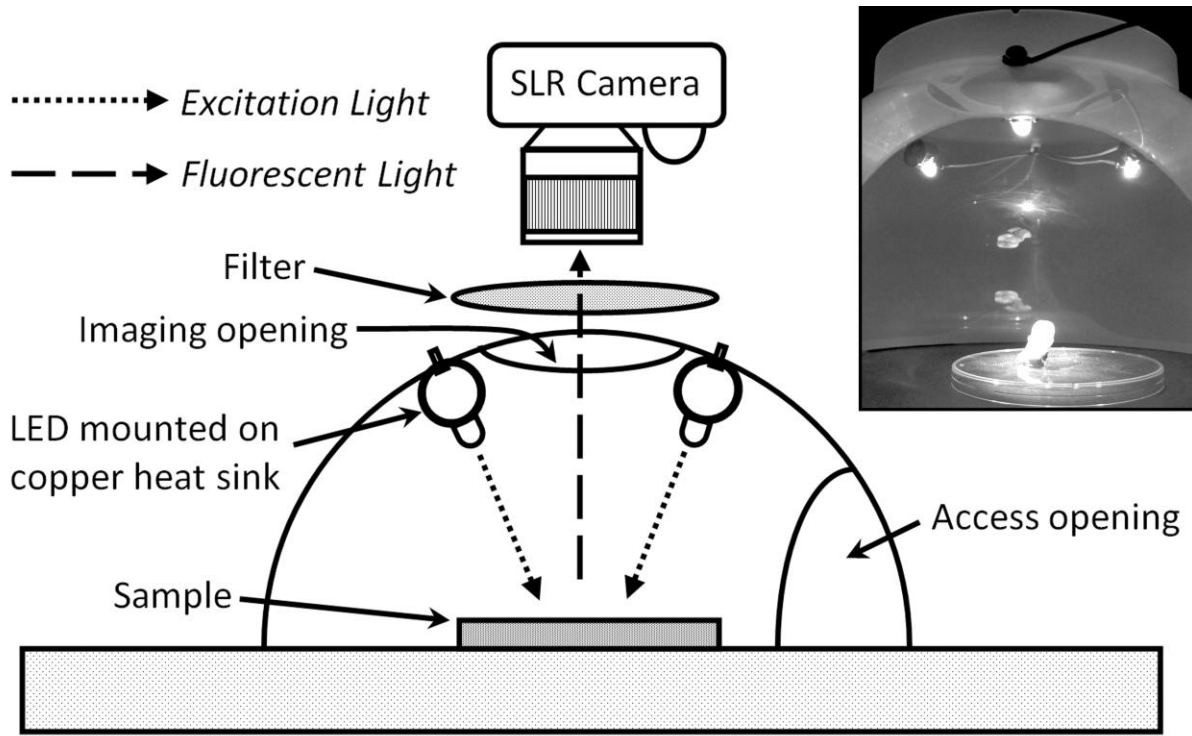
347

348 **Acknowledgments**

349 This work was undertaken as a final year research project by MRTF and was funded
350 internally by the University of Liverpool, School of Dental Sciences and Department
351 of Human Anatomy and Cell Biology.

352

353



355

356

Figure 1. Schematic diagram of the 405 nm lighting rig, comprising of three

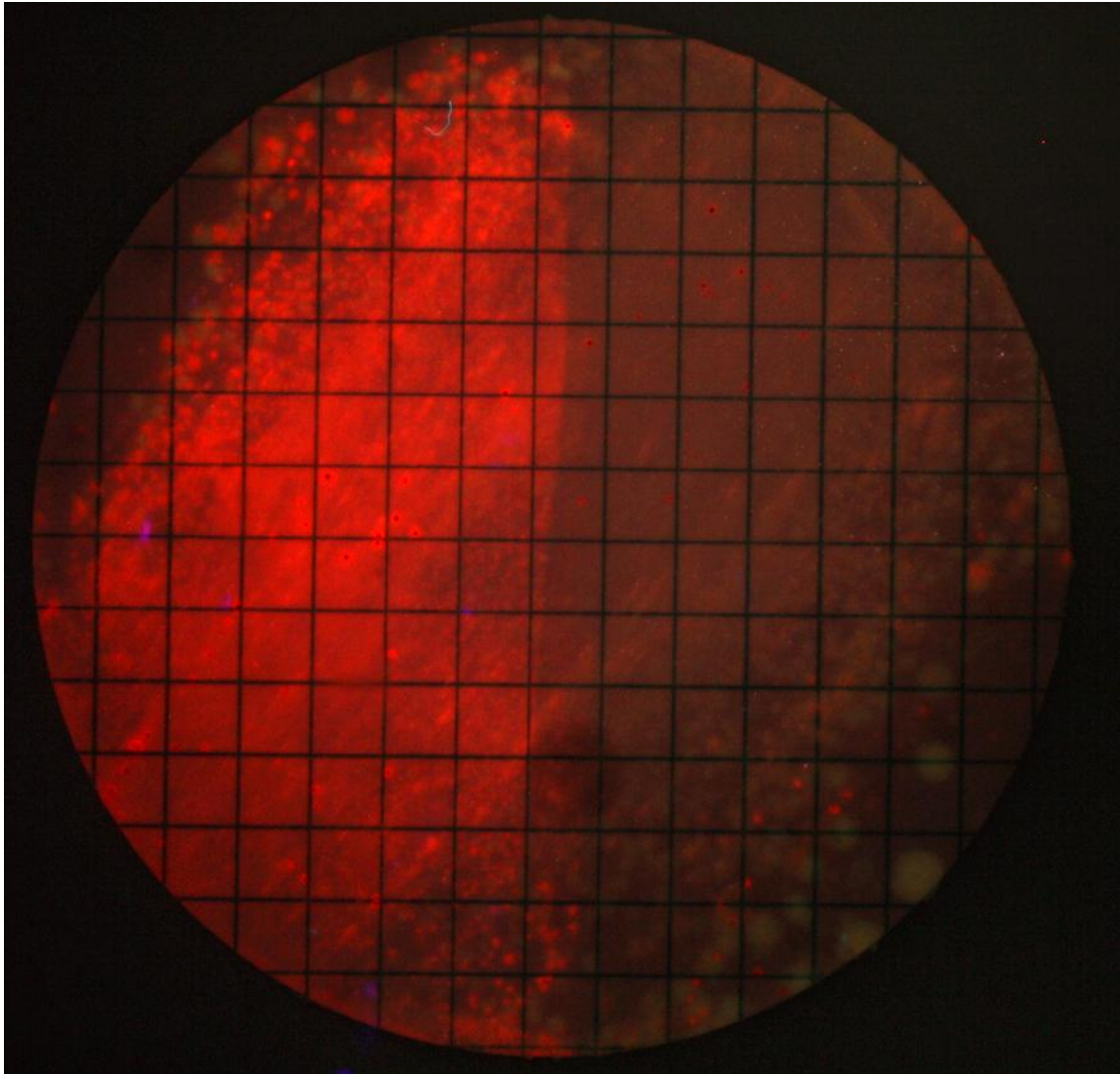
357

equidistant indium gallium nitride light emitting diodes (inset: a tooth sample

358

illuminated by the lighting rig).

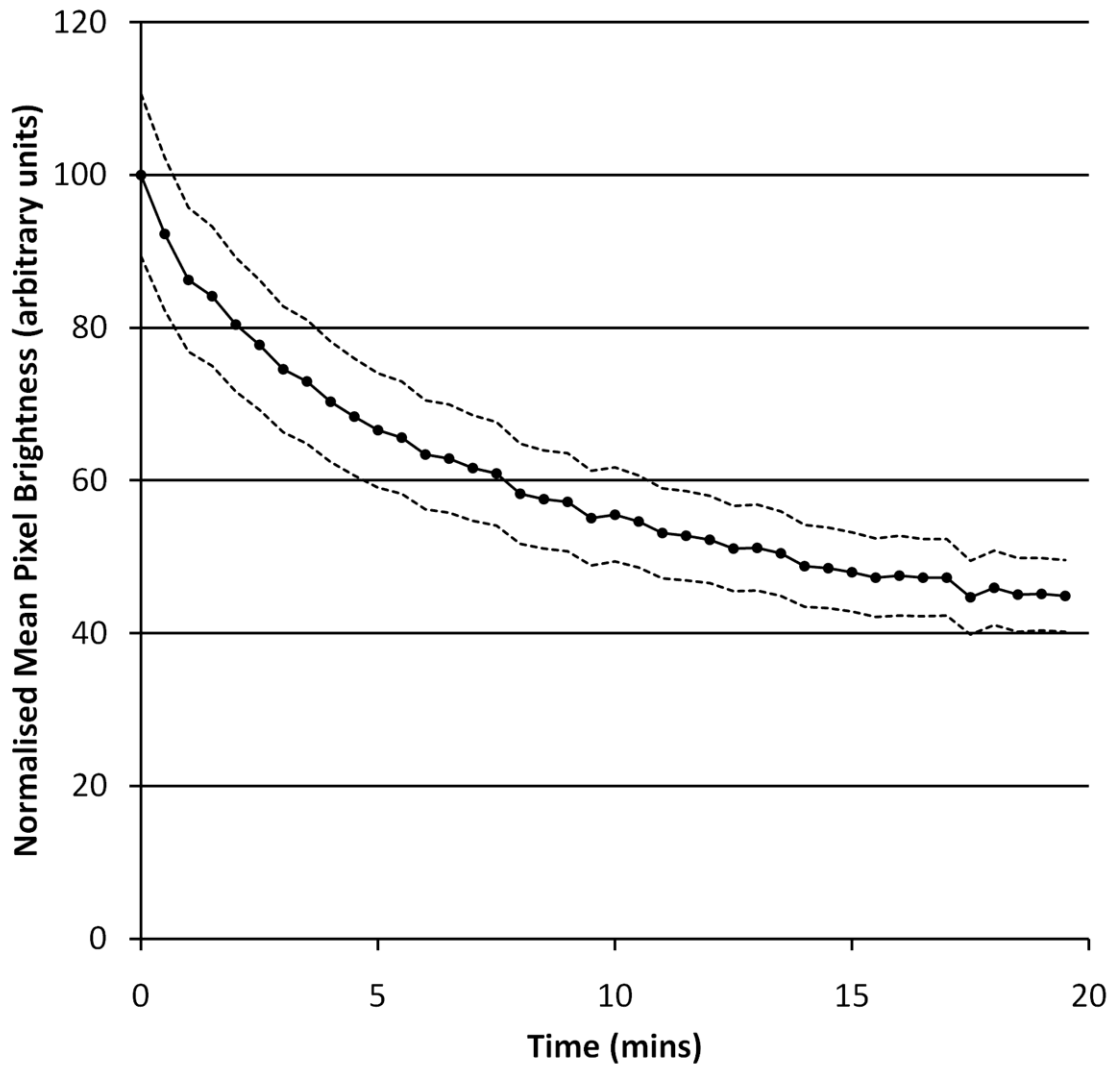
359



360

361 Figure 2. Microcosm filter-membrane biofilm viewed under the QLFD lighting
362 system. Photobleaching was demonstrated on the right-hand side of the membrane
363 in this instance by previously covering the left-hand side of the membrane with
364 aluminium foil whilst 405 nm light at $750 \mu\text{mol m}^{-2} \text{s}^{-1}$ (maximum) was incident onto
365 the sample for 25 minutes. The foil was removed immediately before this image was
366 captured.

367

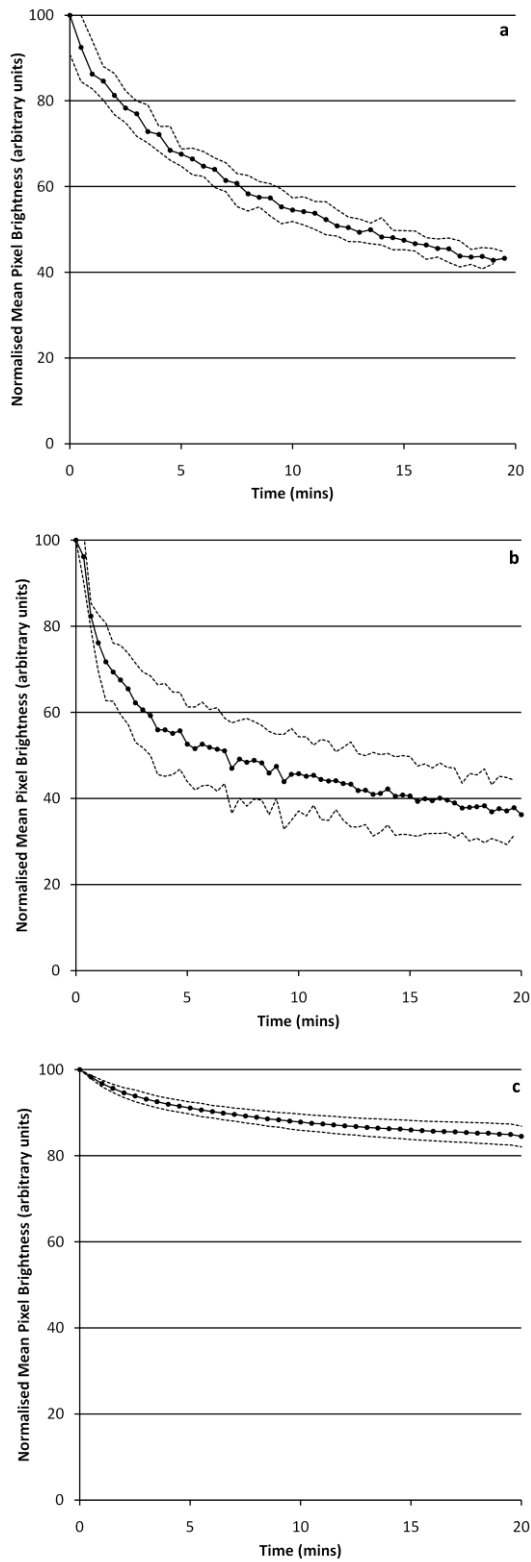


368

369 Figure 3. A representative microcosm biofilm photobleaching experiment following
 370 illumination with the QLFD lighting system. The solid line is the mean pixel
 371 brightness from adjacent regions of interest within the sample (n=8); the dotted lines
 372 show standard deviations.

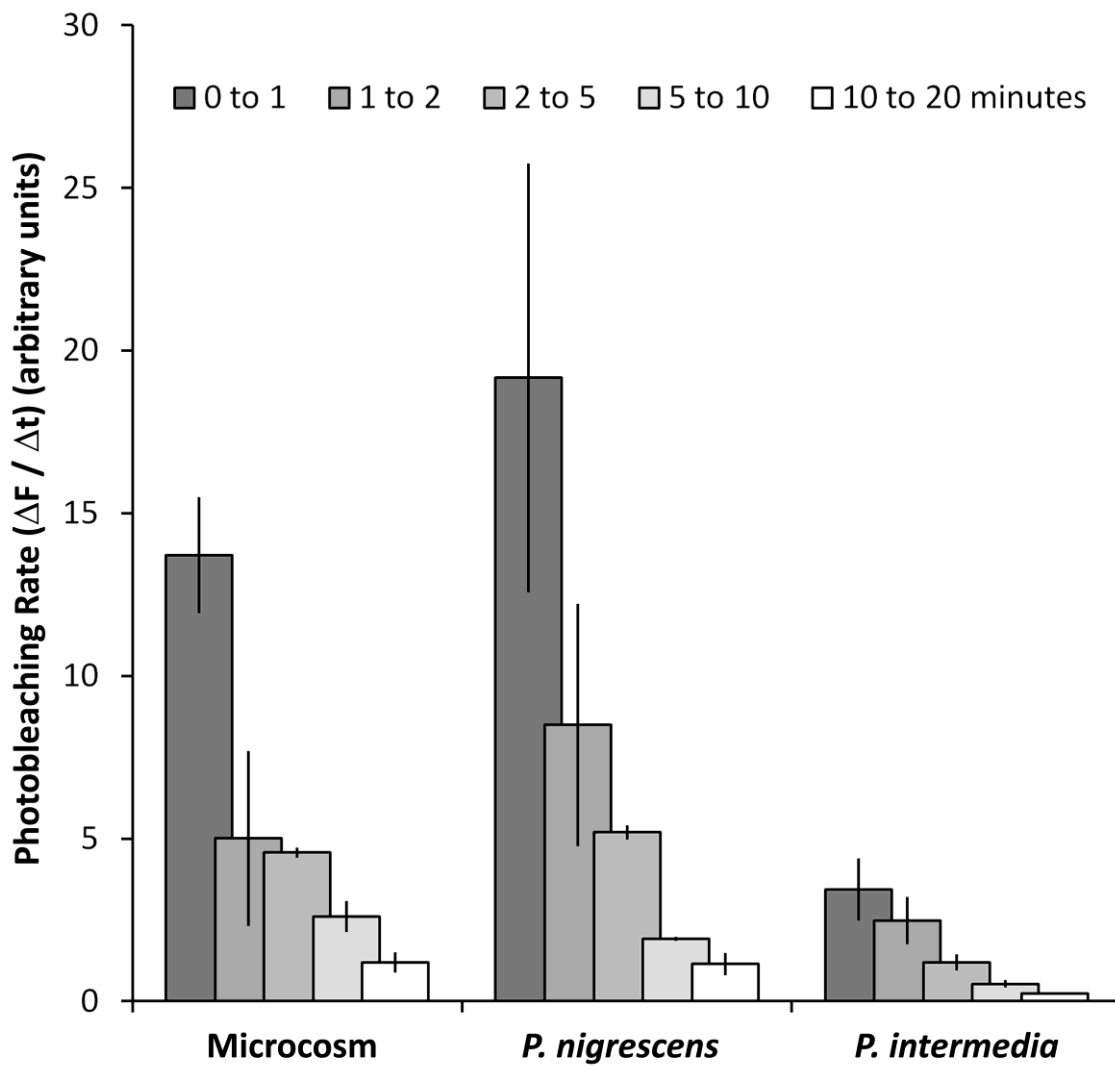
373

374



375

376 Figure 4. Mean red fluorescence observed in microcosm (n=4) (a), *P. nigrescens*
 377 (n=2) (b) and *P. intermedia* (n=2) (c) filter-membrane biofilms viewed under QLFD
 378 lighting. The solid lines represent the mean values with the dotted lines showing
 379 standard deviations.

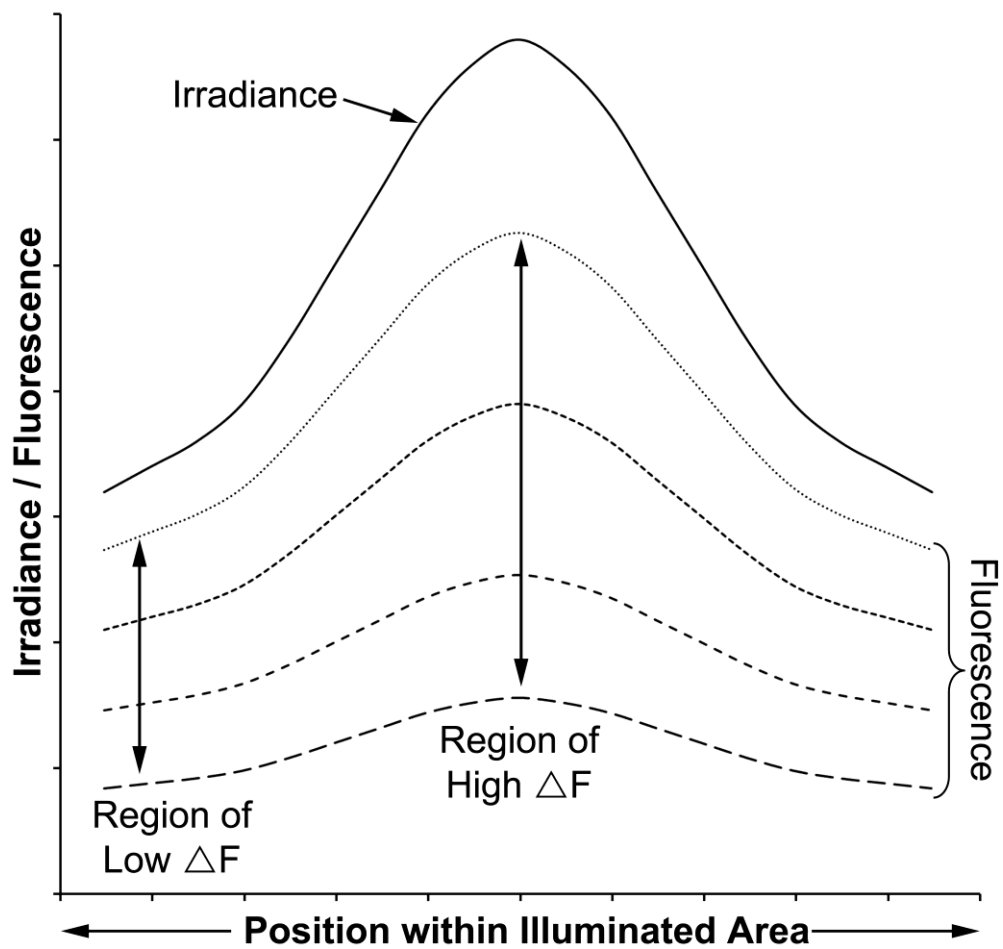


380

381 Figure 5. Rates of photobleaching shown as the decrease in fluorescence (ΔF) with
 382 time (Δt) within a range of time points; 0 to 1, 1 to 2, 2 to 5, 5 to 10 and 10 to 20
 383 minutes. These data corresponds to Figure 4. Error bars indicate standard
 384 deviations.

385

386



387

388 Figure 6. A theoretical model showing differential rates of photobleaching across a
 389 sample illuminated with the custom lighting rig. Heterogenous irradiance of the
 390 sample is represented by the solid line, whereas the resulting fluorescence values
 391 are shown by the dotted lines at four times points. Fluorescence decreases over
 392 time and the rate of photobleaching is directly proportional to the incident irradiation.

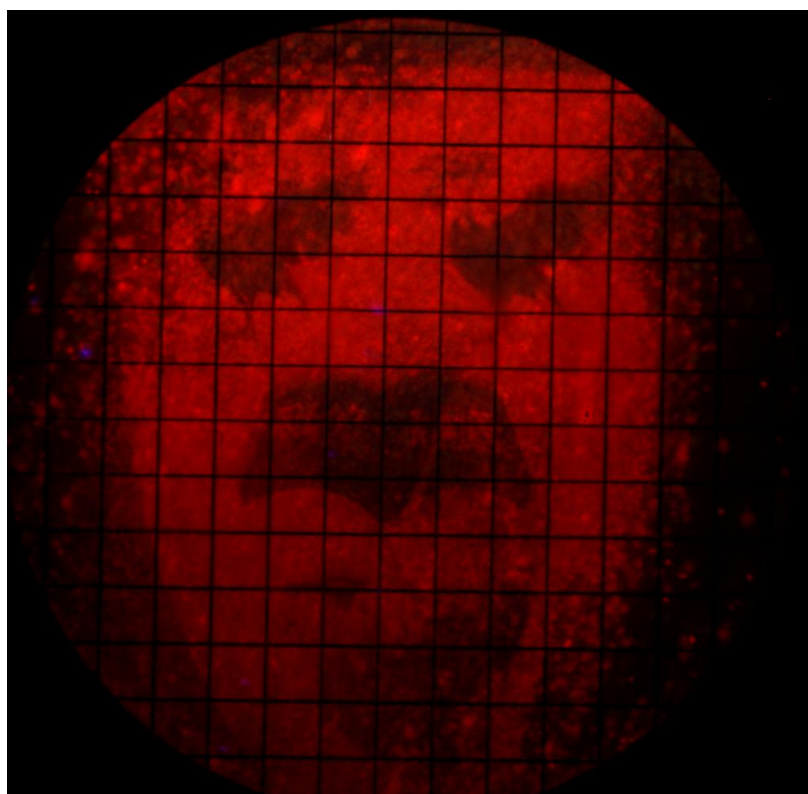
393

394

395



397



398

399

400 **References**

- 401 (1) McGinley KJ, Webster GF, Leyden JJ. Facial follicular porphyrin fluorescence: correlation with
402 age and density of *Propionibacterium acnes*. *BrJ Dermatol* 1980; **102**: 437-441.
- 403 (2) Myers MB, Cherry G, Bornside BB, Bornside GH. Ultraviolet red fluorescence of *Bacteroides*
404 *melaninogenicus*. *Appl Microbiol* 1969; **17**: 760-762.
- 405 (3) Chow AW, Patten V, Guze LB. Rapid screening of *Veillonella* by ultraviolet fluorescence. *J Clin*
406 *Microbiol* 1975; **2**: 546-548.
- 407 (4) Lennon AM, Buchalla W, Brune L, Zimmermann O, Gross U, Attin T. The ability of selected
408 oral microorganisms to emit red fluorescence. *Caries Res* 2006; **40**: 2-5.
- 409 (5) Coulthwaite L, Pretty IA, Smith PW, Higham SM, Verran J. The microbiological origin of
410 fluorescence observed in plaque on dentures during QLF analysis. *Caries Res* 2006; **40**: 112-
411 116.
- 412 (6) Smalley JW, Birss AJ, Silver J. The periodontal pathogen *Porphyromonas gingivalis* harnesses
413 the chemistry of the mu-oxo bishaem of iron protoporphyrin IX to protect against hydrogen
414 peroxide. *FEMS Microbiol Lett* 2000; **183**: 159-164.
- 415 (7) Smalley JW, Silver J, Birss AJ, Withnall R, Titler PJ. The haem pigment of the oral anaerobes
416 *Prevotella nigrescens* and *Prevotella intermedia* is composed of iron(III) protoporphyrin IX in
417 the monomeric form. *Microbiology* 2003; **149**: 1711-1718.
- 418 (8) Shah HN, Collins DM. *Prevotella*, a new genus to include *Bacteroides melaninogenicus* and
419 related species formerly classified in the genus *Bacteroides*. *Int J Syst Bacteriol* 1990; **40**:
420 205-208.
- 421 (9) Lin DL, He LF, Li YQ. Rapid and simultaneous determination of coproporphyrin and
422 protoporphyrin in feces by derivative matrix isopotential synchronous fluorescence
423 spectrometry. *Clin Chem* 2004; **50**: 1797-1803.
- 424 (10) Stokes GG. On the Change of Refrangibility of Light. *Philosophical Transactions of the Royal*
425 *Society of London* 1852; **142**: 463-562.
- 426 (11) Tong-Sheng CS-Q, Z.; Wei, Z.; Qing-Ming, L. A quantitative theory model of a photobleaching
427 mechanism. *Chinese Physics Letters* 2003; **20**: 1940-1943.
- 428 (12) Song L, Varma CA, Verhoeven JW, Tanke HJ. Influence of the triplet excited state on the
429 photobleaching kinetics of fluorescein in microscopy. *Biophys J* 1996; **70**: 2959-2968.
- 430 (13) Soukos NS, Som S, Abernethy AD, et al. Phototargeting oral black-pigmented bacteria.
431 *Antimicrob Agents Chemother* 2005; **49**: 1391-1396.
- 432 (14) Wilson M. Lethal photosensitisation of oral bacteria and its potential application in the
433 photodynamic therapy of oral infections. *PhotochemPhotobiolSci* 2004; **3**: 412-418.
- 434 (15) Koster M, Frahm T, Hauser H. Nucleocytoplasmic shuttling revealed by FRAP and FLIP
435 technologies. *Curr Opin Biotechnol* 2005; **16**: 28-34.
- 436 (16) Bryers JD, Drummond F. Local macromolecule diffusion coefficients in structurally non-
437 uniform bacterial biofilms using fluorescence recovery after photobleaching (FRAP).
438 *Biotechnol Bioeng* 1998; **60**: 462-473.
- 439 (17) Hope CK, Wilson M. Induction of lethal photosensitization in biofilms using a confocal
440 scanning laser as the excitation source. *J Antimicrob Chemother* 2006; **57**: 1227-1230.
- 441 (18) de Josselin de JE, Sundstrom F, Westerling H, Tranaeus S, ten Bosch JJ, ngmar-Mansson B. A
442 new method for in vivo quantification of changes in initial enamel caries with laser
443 fluorescence. *Caries Res* 1995; **29**: 2-7.
- 444 (19) Gmur R, Giertsen E, van dV, de Josselin de JE, Ten Cate JM, Guggenheim B. In vitro
445 quantitative light-induced fluorescence to measure changes in enamel mineralization.
446 *Clin Oral Investig* 2006.
- 447 (20) Ando M, Hall AF, Eckert GJ, Schemehorn BR, Analoui M, Stookey GK. Relative ability of laser
448 fluorescence techniques to quantitate early mineral loss in vitro. *Caries Res* 1997; **31**: 125-
449 131.

- 450 (21) Coulthwaite L, Pretty IA, Smith PW, Higham SM, Verran J. QLF is not readily suitable for in
451 vivo denture plaque assessment. *J Dent* 2009; **37**: 898-901.
- 452 (22) McCree KJ. Significance of Enhancement for Calculations Based on the Action Spectrum for
453 Photosynthesis. *Plant Physiol* 1972; **49**: 704-706.
- 454 (23) Patterson GH, Piston DW. Photobleaching in two-photon excitation microscopy. *Biophys J*
455 2000; **78**: 2159-2162.
- 456 (24) Herzog M, Moser J, Wagner B, Broecker J. Shielding effects and hypoxia in photodynamic
457 therapy. *IntJOral MaxillofacSurg* 1994; **23**: 406-408.
- 458 (25) Rizza V, Sinclair PR, White DC, Cuorant PR. Electron transport system of the protoheme-
459 requiring anaerobe *Bacteroides melaninogenicus*. *J Bacteriol* 1968; **96**: 665-671.
- 460 (26) Lu S, Chen JY, Zhang Y, Ma J, Wang PN, Peng Q. Fluorescence detection of protoporphyrin IX
461 in living cells: a comparative study on single- and two-photon excitation. *J Biomed Opt* 2008;
462 **13**: 024014.
- 463 (27) Slots J, Reynolds HS. Long-wave UV light fluorescence for identification of black-pigmented
464 *Bacteroides* spp. *J Clin Microbiol* 1982; **16**: 1148-1151.
- 465 (28) Shah HN, Bonnett R, Mateen B, Williams RA. The porphyrin pigmentation of subspecies of
466 *Bacteroides melaninogenicus*. *Biochem J* 1979; **180**: 45-50.
- 467 (29) Pretty IA, Edgar WM, Smith PW, Higham SM. Quantification of dental plaque in the research
468 environment. *JDent* 2005; **33**: 193-207.

469

470

471

472